

Learned Fine-Tuner for Incongruous Few-Shot Learning

Pu Zhao¹, Sijia Liu^{2,*}, Parikshit Ram^{2,*}, Songtao Lu², Djallel Bouneffouf², Xue Lin¹

¹ Northeastern University, ² IBM Research

November 24, 2021

Abstract

Model-agnostic meta-learning (MAML) effectively meta-learns an *initialization* of model parameters for few-shot learning where all learning problems share the same format of model parameters – *congruous meta-learning*. We extend MAML to *incongruous meta-learning* where different yet related few-shot learning problems may *not* share any model parameters. A Learned Fine Tuner (LFT) is used to replace hand-designed optimizers (such as SGD) for the task-specific *fine-tuning*. Here, MAML instead meta-learns the parameters of this LFT across incongruous tasks leveraging the learning-to-optimize (L2O) framework such that models fine-tuned with LFT (even from random initializations) adapt quickly to new tasks. As novel contributions, we show that the use of LFT within MAML (i) offers the capability to tackle few-shot learning tasks by meta-learning across incongruous yet related problems (e.g., classification over images of different sizes and model architectures), and (ii) can efficiently work with first-order and derivative-free few-shot learning problems. Theoretically, we quantify the difference between LFT (for MAML) and L2O. Empirically, we demonstrate the effectiveness of LFT through both synthetic and real problems and a novel application of generating universal adversarial attacks across different image sources in the few-shot learning regime.

1 INTRODUCTION

Many machine learning methods are inherently data hungry, requiring large amounts of training examples for improved generalization. This limits the applicability of such methods to problems where only a few examples are available. Meta-learning [1] focuses on leveraging past experiences with similar tasks to “warm-start” the learning on new tasks. In the context of learning neural-networks, *model-agnostic meta-learning* (MAML) [2, 3] focuses on gradient-based learning and meta-learns an initialization for a neural network (for supervised and reinforcement learning) with an **explicit goal of fast adaptation** – the ability to learn a good model with just a few examples (few-shot learning) [4, 5] and a few *fine-tuning* steps (with gradient descent). While the idea of explicitly optimizing for fast adaptation is very general, the practical interpretation of MAML as “parameter initialization” or “reusable parameters” for learning models [6] limits its scope to the situation where the meta-learning and task specific learning (fine-tuning) occurs on the same set of parameters and these parameters are explicitly shared between different tasks. Meta-learning is restricted to tasks that share the same parameter format (for example, parameters of neural networks with the same architecture). We term these as *congruous tasks*.

However, similar tasks with different set of parameters – *incongruous tasks* – such as tasks involving learning networks with different architectures cannot be meta-learned across with MAML. For example, digits image classification, we may use a network with just 3 fully connected layers for one image set (say MNIST [7]) and a network with 3 5x5 convolutional layers and 5 fully connected layers for another image set (say SVHN [8]). Even if the tasks are similar (digits classification), it is not clear

*Equal contribution

how MAML can meta-learn across the parameters of these separate networks. This is because MAML takes advantage of the congruity of the tasks to meta-learn “*where to start learning from with only a few examples*” – this translates to meta-learning initialization for model parameters. We remark that our incongruous setting is different from the ‘heterogeneous’ multi-task setting [9], where the heterogeneity refers to the involvement of different data distributions; the model parameters are still shared and optimized across tasks (heterogeneous yet congruous in our context).

A different application of meta-learning is *learning-to-optimize* (L2O) [10, 11] where the optimization trajectories from different optimization tasks with objectives of different *optimizee* parameters serve as examples for meta-learning the *optimizer* parameters. These learnt optimizers can generalize well to unseen optimization tasks [12, 13], and can train deep learning models better than hand-crafted optimizers such as SGD, RMS-Prop [14] or Adam [15]. Most research has focused on differentiable objectives, but non-differentiable ones can also be handled [16–18].

Learnt optimizers which use gradients or zeroth-order gradient estimates [19, 17] can operate on objectives with *different set of optimizee variables*. This allows meta-learning across incongruous tasks. This meta-learning is distinct for MAML in two ways: (i) MAML is designed for few-shot learning problems while L2O focuses on solving general optimization problems. (ii) More importantly, there is a difference in meta-learning philosophy of these two schemes – while MAML focuses on meta-learning “where to start learning from”, L2O meta-learns “*how to learn*”.

L2O has been used to meta-learn an optimizer/fine-tuner for few-shot tasks [20] – the learned fine-tuner (LFT) is used for task-specific fine-tuning; MAML has been shown to outperform this scheme. This meta-learning was also limited to congruous tasks. We also employ a similar idea of utilizing LFTs for few-shot learning – in contrast to [20], we have significantly different motivations – We interpret MAML as a bi-level learning framework and leverage the L2O framework to explicitly optimize the fast adaptation objective across incongruous few-shot learning tasks. In a way, we explore why and how LFTs enable MAML across incongruous tasks. Our **contributions** demonstrate:

- ▶ (Sec. 2) How meta-learning across incongruous tasks can be formulated as an extended bi-level optimization by integrating L2O into MAML.
- ▶ (Sec. 3) How a learned fine-tuner (LFT) is meta-learned for better generalization in few-shot learning and how LFT theoretically differs from L2O.
- ▶ (Sec. 4) How LFT applies to solving the problem of universal adversarial attack generation in the novel context of meta-learning across incongruous attack generation tasks.
- ▶ (Sec. 5) How our proposed scheme has wider meta-learning applicability than MAML and outperforms L2O for few-shot classification and regression tasks.

2 PROBLEM FORMULATION

In this section, we first review model-agnostic meta learning (MAML) and present its inapplicability to incongruous meta-learning. We then motivate the generalization of MAML to incongruous tasks with LFTs.

Model Agnostic Meta-Learning. MAML meta-learns an initialization of *optimizee* variables θ (e.g., model parameters) that enables fast adaptation to new tasks when fine-tuning the *optimizee* from this learned initialization with only a few new examples. Formally, with N few-shot learning tasks $\{\mathcal{T}_i\}_{i=1}^N$, for meta-learning with task \mathcal{T}_i (a) a fine tuning set $\mathcal{D}_i^{\text{tr}}$ is used for the task-specific *inner loop* in MAML to fine-tune the initial *optimizee* θ , and (b) a validation set $\mathcal{D}_i^{\text{val}}$ is used in the *outer loop* for the evaluating the fine-tuned *optimizee* θ_i^* to meta-update the initialization θ . Thus, MAML

solves the following bi-level optimization problem

$$\begin{aligned} \underset{\theta}{\text{minimize}} \quad & \frac{1}{N} \sum_{i=1}^N \mathbb{E}_{(\mathcal{D}_i^{\text{tr}}, \mathcal{D}_i^{\text{val}}) \sim \mathcal{T}_i} [f_i(\theta_i^*; \mathcal{D}_i^{\text{val}})] \\ \text{subject to} \quad & \theta_i^* = \arg \min_{\theta_i} f_i(\theta_i; \mathcal{D}_i^{\text{tr}}) \end{aligned} \quad (1)$$

where θ_i is the task-specific optimizee and $f_i(\theta_i; \mathcal{D})$ is the task-specific loss evaluated on data \mathcal{D} using variable θ_i obtained from fine-tuning the meta-learned initialization θ . Problem (1) provides a generalized formulation of MAML.

Solving the bi-level program (1) is challenging. In MAML and variants [2, 21, 22], the inner loop is a K-step gradient descent (GD) with the initial $\theta_i^{(0)} = \theta$, the final $\theta_i^* = \theta_i^{(K)}$ and

$$\theta_i^{(k)} = \theta_i^{(k-1)} - \alpha \nabla_{\theta_i} f_i(\theta_i^{(k-1)}; \mathcal{D}_i^{\text{tr}}) \text{ for } k \in [K], \quad (2)$$

where $\theta_i^{(k)}$ is the k^{th} -step optimizee fine-tuned with $\mathcal{D}_i^{\text{tr}}$ from initialization $\theta_i^{(0)} = \theta$, $\alpha > 0$ is a learning rate, and $[K] = \{1, 2, \dots, K\}$. Although GD (2) and variants solve the inner minimization in (1) efficiently, the outer loop requires the second-order derivative with respect to (w.r.t.) θ . With large K , MAML faces the issue of vanishing gradients.

In MAML, both levels of the optimization operate on the same optimizee (for example, same network parameters), and accordingly, learning tasks $\{\mathcal{T}_i\}_{i=1}^N$ are restricted to problems which *share the same optimizee*. However, in the general meta-learning setting, similar tasks could be from related yet *incongruous* domains corresponding to *different objectives* $\{f_i\}$ with optimizee variables of *different dimensions* that cannot be shared between tasks; see a detailed example and illustration in Appendix H. For example, adversarial perturbation parameters cannot be shared between images from different data sources; Network parameters from different architectures cannot be shared even if they are solving related learning tasks. In such cases, meta-learning the initialization is not applicable. Instead, we meta-learn an optimizer – the fine-tuner – for fast adaptation of the task-specific optimizee θ_i in a few-shot setting even when meta-learning across incongruous tasks.

Learning to Optimize (L2O). The L2O framework allows us to replace the hand-designed GD (2) with a learnable recurrent neural network (RNN) parameterized by ϕ . For any task \mathcal{T}_i , the model $\text{RNN}_{\phi}(\cdot)$ mimics a hand-crafted gradient based optimizer to output a descent direction $\Delta\theta_i$ to update task-specific optimizee variable θ_i given the function gradients as input. Thus, we replace (2) with

$$\begin{aligned} \Delta\theta_i^{(k)}, h_i^{(k)} &= \text{RNN}_{\phi} \left(g_i(\theta_i^{(k-1)}; \mathcal{D}_i^{\text{tr}}), h_i^{(k-1)} \right), \\ \theta_i^{(k)} &= \theta_i^{(k-1)} - \Delta\theta_i^{(k)}, \quad \forall k \in [K], \end{aligned} \quad (3)$$

where $h_i^{(k)}$ denotes the state of RNN_{ϕ} at the k^{th} RNN unrolling step, $g_i(\theta_i^{(k)}; \mathcal{D}_i^{\text{tr}})$ represents the gradients $\nabla_{\theta_i} f_i(\theta_i; \mathcal{D}_i^{\text{tr}})$ or gradient estimates [23, 17]. Each task-specific θ_i is randomly initialized.

2.1 Learned Fine-tuners for MAML

We term RNN_{ϕ} in (3) *learned fine-tuner* (LFT) for incongruous few-shot learning. Combining (3) with (1), we can cast the meta-learning of a LFT as

$$\begin{aligned} \underset{\phi}{\text{minimize}} \quad & \widehat{F}(\phi) := \frac{1}{N} \sum_{i=1}^N \mathbb{E}_{(\mathcal{D}_i^{\text{tr}}, \mathcal{D}_i^{\text{val}}) \sim \mathcal{T}_i} \sum_{k=1}^K w_k f_i(\theta_i^{(k)}; \mathcal{D}_i^{\text{val}}) \\ \text{subject to} \quad & \theta_i^{(k)} \text{ is given by (3),} \end{aligned} \quad (4)$$

where w_k is an importance weight for the k^{th} unrolled step in (3). We can set (i) $w_k = 1$ [11], (ii) $w_k = k$ [17], or (iii) $w_k = \mathbb{I}[k = K]$ [13]. Choice (iii) matches the MAML objective (1), focusing on the final fine-tuned solution. However, unlike MAML, problem (4) meta-learns the *fine-tuner* ϕ instead of an initialization θ (Figure A6 vs. A5 visually depict this difference).

Comparison to L2O. Problem (4) is a general version of the meta-learning in L2O where we also meta-learn the *optimizer parameters* Φ . The key difference is the absence of a separate validation set $\mathcal{D}_i^{\text{val}}$ – the fine tuning set $\mathcal{D}_i^{\text{tr}}$ is also used for the outer loop update of the RNN parameters Φ . We theoretically quantify the effect of this difference (Theorem 1), and demonstrate that, in few-shot learning, this leads to significant performance gains. L2O learns Φ by minimizing the fine-tuning loss over the unrolled trajectory. We meta-learn Φ by *directly minimizing the generalization loss* (estimated with $\mathcal{D}_i^{\text{val}}$) over the unrolled trajectory. Our empirical results show that the RNN is able to leverage this difference for improved generalization in both congruous & incongruous few-shot tasks.

Algorithm 1 Meta-learning RNN_Φ with problem (4).

```

1: Input: Tasks  $\{\mathcal{T}_i\}_{i \in [N]}$ , # meta-learning steps  $T$ , # fine-tuning steps per task  $K$ , initial  $\Phi$ ,  $\{\theta_i^{(0)}, h_i^{(0)}\}_{i \in [N]}$ , meta-learning rate  $\beta > 0$ 
2: for  $t \leftarrow 1, 2, \dots, T$  do
3:   for tasks  $i \in$  sampled task batch  $\mathcal{B}_t \subseteq N$  do
4:     sample data  $\mathcal{D}_i^{\text{tr}} \sim \mathcal{T}_i$  for fine-tuning
5:     update task-specific optimizer with  $\mathcal{D}_i^{\text{tr}}$  via (3) for  $K$  steps to obtain  $\{\theta_i^{(k)}\}_{k=1}^K$ 
6:     sample data  $\mathcal{D}_i^{\text{val}} \sim \mathcal{T}_i$  for the meta-update
7:     obtain task-specific gradient w.r.t. fine-tuner parameters  $\Phi$  with  $\mathcal{D}_i^{\text{val}}$ 

$$\mathbf{g}^{(i)} \leftarrow \nabla_{\Phi} \sum_{k=1}^K \left[ w_k f_i(\theta_i^{(k)}; \mathcal{D}_i^{\text{val}}) \right] \tag{5}$$

8:   end for
9:   update fine-tuner  $\Phi$ :  $\Phi \leftarrow \Phi - \beta \sum_{i \in \mathcal{B}_t} \mathbf{g}^{(i)}$ 
10: end for
11: Output:  $\text{RNN}_\Phi$ 

```

3 ALGORITHMIC FRAMEWORK FOR LFT

The meta-learning problem (4) is a bi-level optimization, similar to MAML (1). However, both inner and outer levels are distinct from MAML: In the inner level, we update a task-specific optimizer θ_i by unrolling RNN_Φ for K steps from a *random* initial state $\theta_i^{(0)}$; by contrast, MAML uses GD to update θ_i from the meta-learned initialization (that is, $\theta_i^{(0)} = \theta$). In the outer level, we minimize the objective (4) w.r.t. the optimizer Φ instead of the optimizer initialization θ . We present our proposed scheme in Algorithm 1.

In what follows, we discuss our proposed meta-learning (Alg. 1), showcasing its (i) ability to meta-learn across incongruous tasks, (ii) applicability to zeroth-order (ZO) optimization, (iii) close-formed, recursively computable meta-learning gradient, (iv) theoretical difference from L2O.

Incongruous Meta-learning. When fine-tuning the task-specific optimizer variable θ_i by RNN_Φ (Algorithm 1, Step 6), we can use an *invariant* RNN architecture to tolerate the task-specific variations in the dimensions of optimizer variables $\{\theta_i\}_{i=1}^N$. Recall from (3) that RNN_Φ uses the gradient or gradient estimate $g_i(\theta_i^{(k)}; \mathcal{D}_i^{\text{tr}})$ as an input, which has the same dimension as θ_i . At first glance, a single RNN_Φ seems incapable of handling incongruous $\{\mathcal{T}_i\}_{i=1}^N$ defined over optimizer variables of different dimensionalities. However, a RNN_Φ configured as a *coordinate-wise* Long Short Term Memory (LSTM) network (proposed by Andrychowicz et al. [11]), is invariant to the dimensionality of optimizer variables $\{\theta_i\}_{i=1}^N$ since it independently operates on each coordinate of θ_i regardless of its dimensionality. In contrast to MAML, the invariant RNN_Φ expands the application domain of LFT beyond model weights/parameters over congruous tasks to incongruous ones such as designing universal adversarial perturbations across incongruous attack tasks.

Derivative-free Meta-learning. The use of L2O in (3) also allows us to update the task-specific optimizer variable θ_i using not only first-order (FO) information (gradients) but also zeroth-order

(ZO) information (function values) if the loss function f_i is a black-box objective function. We can estimate the gradient $\nabla f_i(\theta_i; \mathcal{D}_i)$ with finite-differences of function values $g_i(\theta_i; \mathcal{D}_i)$ [19, 17]:

$$g_i(\theta_i; \mathcal{D}_i) = \frac{\sum_{j=1}^n [u_j (f_i(\theta_i + \mu u_j; \mathcal{D}_i) - f_i(\theta_i; \mathcal{D}_i))]}{\mu n}, \quad (6)$$

where $\mu > 0$ is a small smoothing parameter, $u_j, j \in [n]$ are n random directions with entries from $\mathcal{N}(0, 1)$. This gives us ZO-LFT alongside our original FO-LFT. The function g_i can also be sophisticated quantities derived from gradients as proposed in [12, 13, 18].

The support for ZO optimization is crucial when explicit gradient expressions are computationally difficult or infeasible. Our experiments show that ZO-LFT can be as effective as state-of-the-art FO-LFT, despite leveraging only the inputs and outputs of the DL model (see Figure 3 in Section 5).

Meta-learning Gradient. Since Algorithm 1 meta-learns the optimizer variable Φ rather than the initialization of optimizee variable θ , it requires a different meta-learning gradient $\nabla_{\Phi} \sum_k w_k f_i(\theta_i^{(k)}, \mathcal{D}_i^{\text{val}})$. Focusing only on $\nabla_{\Phi} f(\theta^{(k)}; \mathcal{D}^{\text{val}})$ in (5) and dropping the task index i :

$$\nabla_{\Phi} f(\theta^{(k)}; \mathcal{D}^{\text{val}}) = \underbrace{\frac{\partial f(\theta^{(k)}; \mathcal{D}^{\text{val}})}{\partial \theta}}_{g(\theta^{(k)}; \mathcal{D}^{\text{val}})} \bullet \underbrace{\frac{\partial \theta^{(k)}}{\partial \Phi}}_{G^{(k)}} \quad (7)$$

where \bullet denotes a matrix product that the chain rule obeys [24]. Statement 1 details the recursive computation of $G^{(k)}$, which calls for the second-order (or first-order) derivative of f w.r.t. θ if $g(\theta^{(k)}; \mathcal{D}^{\text{tr}})$ denotes the gradient (or gradient estimate) of f in (3). We refer readers to Appendix A for the details of derivation.

Statement 1 *Given the RNN update rule in (3), denote $g(\theta; \mathcal{D}^{\text{tr}})$ as $g(\theta)$, $\Delta \theta^{(k)} = \Gamma(\Phi, g(\theta^{(k-1)}), h_{k-1})$, $h_k = \Pi(\Phi, g(\theta^{(k-1)}), h_{k-1})$ and $H^{(k)} = \frac{\partial h_k}{\partial \Phi}$. Then $G^{(k+1)} = \partial \theta^{(k+1)} / \partial \Phi$ is defined as*

$$G^{(k)} = \frac{\partial \Gamma(\Phi, g, h_k)}{\partial g} \Big|_{g=g(\theta^{(k)})} \bullet \frac{\partial g(\theta)}{\partial \theta} \Big|_{\theta=\theta^{(k)}} \bullet G^{(k)} - \frac{\partial \Gamma(\Phi, g(\theta^{(k)}), h)}{\partial h} \Big|_{h=h_k} \bullet H^{(k)} - \frac{\partial \Gamma(\Phi, g(\theta^{(k)}), h_k)}{\partial \Phi}, \quad (8)$$

and $H^{(k+1)}$ is defined as

$$\frac{\partial \Pi(\Phi, g(\theta^{(k)}), h_k)}{\partial \Phi} + \frac{\partial \Pi(\Phi, g(\theta^{(k)}), h)}{\partial h} \Big|_{h=h_k} \bullet H^{(k-1)} + \frac{\partial \Pi(\Phi, g, h_k)}{\partial g} \Big|_{g=g(\theta^{(k)})} \bullet \frac{\partial g(\theta)}{\partial \theta} \Big|_{\theta=\theta^{(k)}} \bullet G^{(k)}. \quad (9)$$

It is clear from (8) and (9) that the second-order derivatives are involved without additional assumptions due to the presence of $\frac{\partial g(\theta^{(k-1)})}{\partial \theta}$ if $g(\theta^{(k-1)})$ is specified by the first-order derivative w.r.t. θ ; only first-order derivatives are involved when working with ZO gradient estimates. With the use of the coordinate-wise RNN, the terms $\frac{\partial \Gamma}{\partial g}$, $\frac{\partial \Gamma}{\partial h}$, $\frac{\partial \Pi}{\partial g}$, $\frac{\partial \Pi}{\partial h}$ correspond to diagonal matrices. Note that $G^{(0)} = 0$ and $H^{(0)} = 0$. Unlike MAML, this recursively defined meta-learning gradient w.r.t. Φ is not as prone to the issue of vanishing gradients for large values of K .

Theoretical Analysis. L2O is empirically very capable of meta-learning from optimization trajectories, with better convergence than hand-crafted optimizers. Using notation from Sec. 2, the L2O objective can be written as:

$$\begin{aligned} \min_{\Phi} \quad & F(\Phi) = \frac{1}{N} \sum_{i=1}^N \mathbb{E}_{\mathcal{D}_i^{tr} \sim \mathcal{T}_i} \left\{ \sum_{k=1}^K \left[w_k f_i(\theta_i^{(k)}; \mathcal{D}_i^{tr}) \right] \right\} \\ \text{s.t.} \quad & \theta_i^{(k)} \text{ defined as (3)}. \end{aligned} \quad (10)$$

Under standard assumptions, we show the following result, quantifying the difference between L2O and our proposed meta-learning with respect to the size of the meta-learning gradient w.r.t. Φ in Algorithm 1 (Appendix B):

Theorem 1 *Consider the meta-learning objectives defined in (4) and (10). Suppose that the gradient size is bounded by G and gradient estimate per sample has uniformly bounded variance σ^2 . Then, for any Φ , we have*

$$\left\| \nabla_{\Phi} F(\Phi) - \nabla_{\Phi} \hat{F}(\Phi) \right\| \leq \sqrt{2} G \sigma \sqrt{\frac{1}{D_{tr}} + \frac{1}{D_{val}}} \quad (11)$$

where $D_{tr} := \min_{i \in [N]} |\mathcal{D}_i^{tr}|$ and $D_{val} := \min_{i \in [N]} |\mathcal{D}_i^{val}|$ denote the minimum batch size of per-task datasets $\mathcal{D}_i^{tr}, \mathcal{D}_i^{val} \sim \mathcal{T}_i, i \in [N]$.

Remark 1 *When D_{tr} and D_{val} are both large enough the difference between L2O and our proposed meta-learning is small. In this case, we reduce to L2O. From previous works, we know that L2O can meta-learn optimizers with good convergence properties, implying that our LFTs would also converge to similar results by leveraging the RNN structure.*

Remark 2 *When the data size is small – the few-shot learning regime – there could be a gap between the two frameworks, resulting in a significant difference in the solutions generated by L2O and our scheme, especially for the case where σ or G is large. This explains the significant difference between the empirical performance of L2O and our LFTs in the evaluation over few-shot learning problems in Secs. 4 & 5. The effect of the batch sizes D_i^{tr}, D_i^{val} on the difference in performance is presented in Appendix F, validating the theory.*

4 APPLICATION: ADVERSARIAL ATTACK AGAINST HYBRID IMAGE SOURCES

Recent research demonstrates the lack of robustness of deep neural network (DNN) models against *adversarial perturbations/attacks* [25–28] – imperceptible perturbations to input examples (e.g. images) – crafted to manipulate the DNN prediction. The problem of *universal adversarial perturbation* (UAP) seeks a *single* perturbation pattern to manipulate the outputs of the DNN to *multiple examples simultaneously* [29]. Often, this universal perturbation is learned with a set of “training” examples and then applied to unseen “test” examples. However, learning perturbations in a *few-shot* setting with just a few examples, while being able to successfully attack unseen examples is very challenging.

Specifically, the attacker aims to fool a well-trained DNN by perturbing input images with the UAP. Let $p(x)_c$ denote the probability predicted by the DNN for input x and class c . Given a task-specific data set \mathcal{D}_i (corresponding to a task \mathcal{T}_i), the design of UAP θ_i is cast as

$$\underset{\theta}{\text{minimize}} \quad f_i(\theta_i, \mathcal{D}_i) := \sum_{(x,y) \in \mathcal{D}_i} \ell_{\text{atk}}(\theta_i, x, y) + \lambda \|\theta_i\|_1, \quad (12)$$

where y is the true label of x , $\lambda > 0$ is a regularization parameter, and ℓ_{atk} is the C&W attack loss [27], which is 0 (indicating a successful attack) when the incorrect class $c \neq y$ is predicted as the top-1 class. The second term of (12) is an ℓ_1 regularizer, which penalizes the perturbation strength of θ , measured by its ℓ_1 norm.

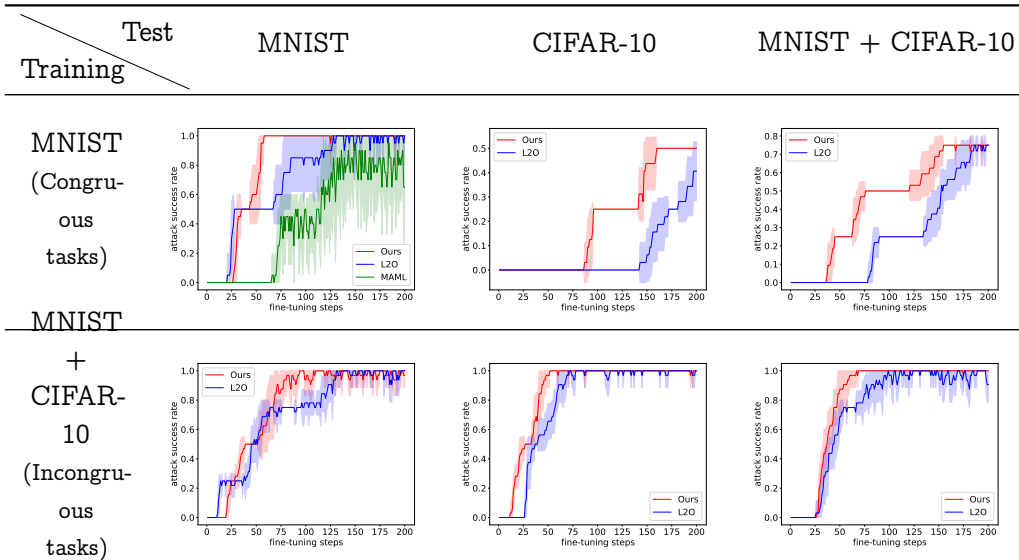


Figure 1: ASR of UAP learnt by LFT, MAML, L2O in various training & evaluation settings. The rows represent the meta-training with congruous (row 1) & incongruous tasks (row 2). The columns represent settings of meta-test tasks. Each cell presents ASR of UAP generated by the scheme meta-learned in the row-specific setting but meta-tested in the column-specific setting with increasing fine-tuning steps. Plots in each cell present the average (solid) \pm standard deviation (shaded) ASR over 100 tasks.

Meta-learning for UAP generation. A direct solution to problem (12) *only* ensures the attack power of UAP (θ_i) against the given data set \mathcal{D}_i at the specific task \mathcal{T}_i . Like any learning problem, the set \mathcal{D}_i needs to be large for the UAP to successfully attack unseen examples. In the few-shot setting (small \mathcal{D}_i), we want to leverage meta-learning to facilitate better generalization for the learned UAP. The attack loss (12) is considered as the task-specific loss f_i in (4) with θ_i as the optimizee. With multiple few-shots tasks \mathcal{T}_i & corresponding $(\mathcal{D}_i^{\text{tr}}, \mathcal{D}_i^{\text{val}})$, we meta-learn the fine-tuner RNN_ϕ to generate UAPs for new few-shot UAP tasks. For comparison, we also consider (i) MAML to meta-learn an initial UAP θ for each task, and (ii) L2O to meta-learn RNN_ϕ for just solving (12). Experiments are conducted over two types of tasks:

- (a) *Congruous* tasks: Tasks are drawn from the *same* dataset (MNIST). In this setting, the applicable methods include LFT, MAML, and L2O. We use MAML here since we can have a UAP parameter that is shared across all tasks. We consider MAML [2] rather than [20] in meta learning over congruous tasks since the former has been shown to have an improved performance over the latter.
- (b) *Incongruous* tasks: Tasks are drawn from a union of *different* image sources (in this case MNIST & CIFAR-10). Unlike (a), it is not possible to share UAP parameters across all tasks from different image sets. Hence MAML is not applicable.

Experimental Setting. We meta-learn LFT, MAML and L2O with 1000 few-shot UAP tasks $\{\mathcal{T}_i\}$. In LFT and MAML, the fine-tuning and meta-update sets $(\mathcal{D}_i^{\text{tr}}, \mathcal{D}_i^{\text{val}}) \sim \mathcal{T}_i$ are drawn from the training dataset and the test dataset of an image source, respectively. However, both MNIST and CIFAR-10 are used across tasks. In both $\mathcal{D}_i^{\text{tr}}$ & $\mathcal{D}_i^{\text{val}}$, 2 image classes with 2 samples per class are randomly selected. In L2O, $\mathcal{D}_i^{\text{tr}}$ is combined with $\mathcal{D}_i^{\text{val}}$; there is no meta-validation involved in the meta-learning. We evaluate the performance of the meta-learning schemes over 100 random unseen few-shot UAP tasks (data for task is generated in a manner described above). Moreover, both LFT and L2O are fine-tuned from random initialization over test tasks; MAML, when applicable, starts fine-tuning with the meta-learned initialization. We refer readers to Appendix C for more details.

Overall Performance. We evaluate the performance of LFT to tackle attack tasks involving different image sets (such as MNIST & CIFAR10). We report the averaged attack success rate (ASR), ℓ_1 -norm

distortion, and number of fine-tuning steps required to first reach 100% ASR (within 200 steps) of generated UAP using different meta-learners (LFT, MAML, L2O), where the victim DNN is given by the LeNet-5 model [30].

We summarize the key performance statistics as below, but refer readers to Table ?? for detailed results. Compared to MAML and L2O, we find that LFT yields an UAP generator with fastest adaption (24%-55% reduction in fine-tuning step # required to first reach 100% ASR), and highest ASR (15% improvement in congruous tasks and 8%-25% improvement in incongruous tasks). Moreover, we find that the improved attack performance is *not* at the cost of increasing distortion strength (in terms of ℓ_1 norm). In fact, LFT yields the lowest attack distortion at most of the time.

Detailed Results. In Figure 1, we focus on analyzing ASR of UAP over test tasks versus the number of fine-tuning steps. We present ASR at every combination of training and evaluation settings, denoted by the pair of datasets. For example, (MNIST, CIFAR-10) implies that meta-learning is performed with MNIST and then used to generate UAP against CIFAR-10 at (meta-)testing. And we use MNIST + CIFAR-10 to represent the union of MNIST and CIFAR-10 tasks for meta-learning (or meta-testing).

We find that LFT outperforms MAML and L2O when meta-learning *and* meta-testing with congruous UAP tasks, namely, (MNIST, MNIST) in Figure 1. The improvement lies at three aspects. (i) Fewest fine-tuning steps are required to attack new tasks with 100% ASR; (ii) Highest ASR can be achieved at a given number of fine-tuning steps; (iii) Lowest perturbation strength is needed to achieve the most significant attacking power (Figure A1) We also note that L2O yields better performance (higher ASR and lower distortion) than MAML. This indicates that in these few-shot UAP tasks, the “how to learn” seems more useful than “where to learn from”.

On the other hand, LFT outperforms L2O in the standard transfer attack settings, corresponding to the scenario (MNIST, CIFAR-10) in Figure 1, where the generator of UAP is learnt over MNIST, but tested over CIFAR-10. Note that MAML can not be applied to this scenario, since the meta-learned UAP initialization does not have the same dimension as the test data. Compared to the congruous setting (MNIST, MNIST), the ASR decreases from 100% to 50% for LFT and L2O. However, LFT adapts better to unseen tasks.

Lastly, LFT outperforms L2O in cases that involve incongruous tasks drawn from MNIST + CIFAR-10. One interesting observation is that the use of hybrid data sources (incongruous tasks) during meta-training enables the learned fine-tuner to generate UAP with faster adaptation on unseen images; compare rows 1 & 2 of Figure 1. In Figure A2, A3 and A4 of Appendix E, we present additional results on the validation loss of LFT, comparison to white-box attacks, and visualization of UAP patterns.

5 EXPERIMENTS IN FEW-SHOT CLASSIFICATION AND REGRESSION

Image Classification Using Hybrid DNN Models. In this experiment, we consider to learn DNN-based image classifiers over 2-way 5-shot learning tasks. These tasks are drawn from two image sources, MNIST & CIFAR-10. We specify the classifier to be trained as a 3-layer multilayer perceptron (MLP) for MNIST data and a convolutional neural network (CNN) with four CONV layers for CIFAR-10 data. Thus, the task-specific optimizer in (4) corresponds to the DNN parameters for a given task. The incongruous tasks are then given by learning DNNs with different architectures (MLP and CNN). We also consider the congruous setting where only one model architecture is adopted across tasks.

In Table 1, we evaluate the classification accuracy of the model parameters acquired from LFT, MAML and L2O over 500 randomly selected 2-way 5-shot test tasks. Here tasks acquired from different data sources (MNIST or CIFAR-10) correspond to different model architectures (MLP or CNN). Our proposed LFT is able to match MAML for congruous tasks (meta-learning with tasks from (CIFAR-10, CNN) and meta-testing with tasks from same set). MAML is not applicable for the incongruous tasks

Table 1: Averaged test accuracy \pm standard deviation for different classifiers acquired from different meta-learners, MAML, L2O, and our proposed LFT, in each paired meta-training and testing configuration. Here the merged ‘Training’ columns show training data sources (implying different model architectures – MLP for MNIST tasks & CNN for CIFAR-10 tasks) and meta-learning methods. Similarly, the merged ‘Testing’ rows show data sources of test tasks as well as the associated model architectures. Note that MAML is *not applicable* (N/A) to incongruous tasks across multiple architectures and datasets.

Training \ Testing		Testing		
		(MNIST, MLP)	(CIFAR-10, CNN)	(MNIST, MLP) + (CIFAR-10, CNN)
(CIFAR-10, CNN)	MAML	N/A	66% \pm 0.8%	N/A
	L2O	27% \pm 2.1%	63% \pm 1.4%	44% \pm 1.4%
	LFT	35% \pm 1.9%	66% \pm 1.3%	47% \pm 1.5%
(MNIST, MLP) + (CIFAR-10, CNN)	MAML	N/A	N/A	N/A
	L2O	81% \pm 1.0%	53% \pm 1.2%	68% \pm 1.1%
	LFT	83% \pm 0.9%	57% \pm 1.3%	72% \pm 1.2%

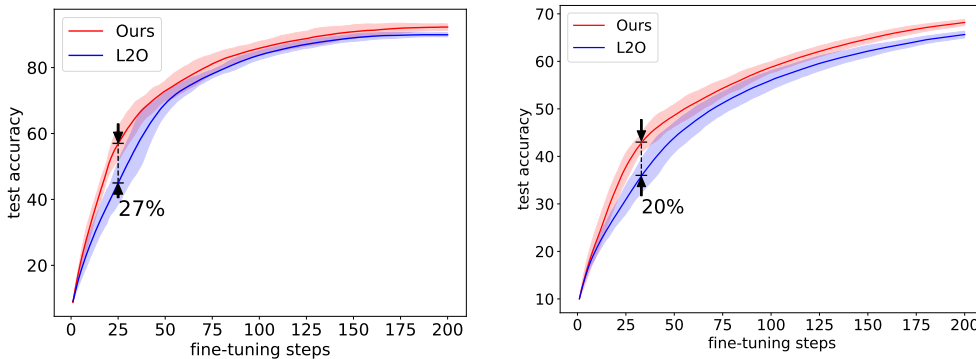


Figure 2: Few-shot test accuracy learnt by LFT and L2O over 500 tasks for different fine-tuning steps. (Left) meta-test tasks from MNIST. (Right) meta-test tasks from CIFAR-10. The incongruous few-shot tasks from MNIST & CIFAR-10 are considered during meta-training. The plots present the averaged accuracy \pm standard deviation over the test tasks.

(at meta-learning or meta-testing). L2O and LFT are applicable, and LFT achieves higher accuracy ($> 2 - 8\%$) throughout. Figure 2 shows that LFT can outperform L2O by up to 20% or more when considering a smaller number of fine-tuning steps.

Furthermore, in Table A2, we compare LFT with L2O and MAML for tackling 5-way 5-shot congruous/incongruous tasks defined over Omniglot and MiniImagenet datasets. We assign two CNN models to Omniglot- and MiniImagenet-related tasks: CNN with 2 CONV layers for Omniglot tasks, and CNN with 4 CONV layers for MiniImagenet tasks. Similar to results in Table 1 we observe that LFT outperforms L2O and MAML in the congruous setting (Omniglot, Omniglot) as well as the other incongruous task settings. It is worth mentioning that the accuracy of MAML (93%) is lower than that of the accuracy (98%) reported in [2] since a different CNN architecture is considered in our experiments.

Application to Supervised Regression. In the next experiment, we revisit the sine wave regression problem presented in MAML [2, Sec. 5.1]. Here multiple few-shot regression tasks are generated by randomly varying the amplitude and the phase of a sinusoid. The goal is to learn a regression model to gain fast adaption from observed few-shot regression tasks to unobserved regression tasks. We find that LFT outperforms L2O and MAML, and the use of ZO-LFT could be as effective as FO-LFT. We

Table 2: Averaged test accuracy \pm standard deviation for different CNN classifiers acquired from different meta-learners, MAML, L2O, and LFT under various meta-training and testing configurations (similar to Table 1) but under Omniglot and MiniImagenet datasets.

Training \ Testing		Omniglot	MiniImagenet	Omniglot + MiniImagenet
Omniglot	MAML	93% \pm 0.7%	N/A	N/A
	L2O	89% \pm 0.9%	17% \pm 1.8%	42% \pm 1.7%
	LFT	94% \pm 0.8%	19% \pm 2.1%	46% \pm 1.4%
Omniglot + MiniImagenet	MAML	N/A	N/A	N/A
	L2O	85% \pm 1.3%	41% \pm 1.8%	57% \pm 1.5%
	LFT	89% \pm 1.0%	45% \pm 1.9%	62% \pm 1.4%

refer readers to Appendix G for more details on experiment setup. Figure 3 presents the few-shot test mean squared error (MSE) versus the fine-tuning iterations. We report the performance of both FO and ZO variants of meta-learners based on gradient and gradient estimates, respectively. As we can see, LFT outperforms L2O and MAML, and the use of ZO-LFT could be as effective as FO-LFT.

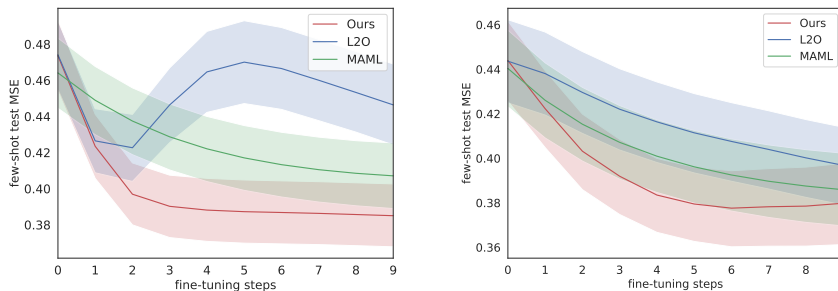


Figure 3: Few-shot test MSE of regressor fine-tuned by the learnt LFT, L2O and MAML over 500 regression tasks for different fine-tuning steps. (Left) FO learning setting. (Right) ZO learning setting. The plots present the averaged MSE over all test tasks together with its standard deviation.

6 RELATED WORK

MAML has been extremely useful in supervised and reinforcement learning (RL), and has been “reframed as a graphical model inference problem” that allows for modeling uncertainty [31]. Grant et al. [32] provide a closely related but distinct interpretation of MAML as “inference for the parameters for a prior distribution in a hierarchical Bayesian model”. The higher order derivatives through the fine-tuning trajectory and the consequent vanishing gradients during the meta-learning is addressed with “implicit gradients” that only depend on the final fine-tuned result [33]. Specific to RL, various enhancements obviate the second order derivatives of the RL reward function, such as variance reduced policy gradients [34] and Monte Carlo zeroth-order Evolution Strategies gradients [35].

MAML requires access to the computationally expensive second-order information of the loss. Fallah et al. [36] study FO-MAML which ignores the second-order term and shows that if the fine-tuning learning rate α is small or the tasks are statistically “close” to each other, the first-order approximation induces negligible error. They also propose HF-MAML, which recovers the guarantees for MAML while avoiding the Hessian computation. Yao et al. [9] propose a hierarchically structured meta-learning (HSML) algorithm that explicitly tailors the transferable knowledge to different task clusters. The core idea is to perform cluster-specific meta-learning, resulting in tighter generalization bounds. Ji et al. [37] present a Hessian-free MAML with multiple fine-tuning steps.

Learnt optimizers have long been considered in the context of training neural networks [38–40].

More recent work has posed optimization *with gradients* as a reinforcement learning problem [10] or as learning a recurrent neural network (RNN) [11] instead of leveraging the usual hand-crafted optimizers (such as SGD, RMSProp [14], Adam [15]). The RNN based optimizers have been improved [12, 13] by – (i) utilizing hierarchical RNNs that capture the parameter structure in the optimization of DL models, (ii) using hand-crafted-optimizer-inspired inputs to the RNN (such as momentum), and (iii) using a diverse set of optimization objectives (with different hardness levels) to train the RNN. The learnt optimizers have also been successful with particle swarm optimization [18] and zeroth-order gradient estimates [17]. However, at this point, there are no theoretical guarantees for learnt optimizers.

7 CONCLUSION

MAML meta-learns an effective initialization of model parameters in few-shot learning. In this paper, we generalize MAML to *incongruous few-shot learning* by replacing the hand-designed optimizer in the inner fine-tuning loop of MAML with a learned fine-tuner (LFT) in the form of a recurrent neural network (RNN). We show that the LFTs can be meta-learned across incongruous tasks and then applied to few-shot problems. We also theoretically quantify the difference between our proposed meta-learning scheme and L2O, highlighting why our proposed meta-learning scheme would outperform L2O for incongruous few-shot learning. Empirically, we consider a novel application of meta-learning to generate universal adversarial perturbations and show the superior performance of our LFTs over the state-of-the-art meta-learners. We also show how our LFTs outperform existing meta-learning schemes for incongruous few-shot classification and regression (when applicable).

References

- [1] Joaquin Vanschoren. Meta-learning: A survey. *arXiv preprint arXiv:1810.03548*, 2018.
- [2] Chelsea Finn, Pieter Abbeel, and Sergey Levine. Model-agnostic meta-learning for fast adaptation of deep networks. *arXiv preprint arXiv:1703.03400*, 2017.
- [3] Z. Zhuang, Y. Wang, K. Yu, and S. Lu. No-regret non-convex online meta-learning. In *Proc. of IEEE International Conference on Acoustics, Speech and Signal Processing*, pages 3942–3946, 2020.
- [4] Yaqing Wang, Quanming Yao, James T. Kwok, and Lionel M. Ni. Generalizing from a few examples: A survey on few-shot learning. *ACM Comput. Surv.*, 53(3), June 2020. ISSN 0360-0300. doi: 10.1145/3386252. URL <https://doi.org/10.1145/3386252>.
- [5] D. Das and C. S. G. Lee. A two-stage approach to few-shot learning for image recognition. *IEEE Transactions on Image Processing*, 29:3336–3350, 2020.
- [6] Aniruddh Raghu, Maithra Raghu, Samy Bengio, and Oriol Vinyals. Rapid learning or feature reuse? towards understanding the effectiveness of maml. *ICLR*, 2020.
- [7] Yann LeCun. The mnist database of handwritten digits. <http://yann.lecun.com/exdb/mnist/>, 1998.
- [8] Yuval Netzer, Tao Wang, Adam Coates, Alessandro Bissacco, Bo Wu, and Andrew Y Ng. Reading digits in natural images with unsupervised feature learning. *NIPS Workshop on Deep Learning and Unsupervised Feature Learning*, 2011.
- [9] Huaxiu Yao, Ying Wei, Junzhou Huang, and Zhenhui Li. Hierarchically structured meta-learning. *arXiv preprint arXiv:1905.05301*, 2019.
- [10] Ke Li and Jitendra Malik. Learning to optimize. *ICLR*, 2017.
- [11] Marcin Andrychowicz, Misha Denil, Sergio Gomez, Matthew W Hoffman, David Pfau, Tom Schaul, Brendan Shillingford, and Nando De Freitas. Learning to learn by gradient descent by gradient descent. In *Advances in neural information processing systems*, pages 3981–3989, 2016.
- [12] Olga Wichrowska, Niru Maheswaranathan, Matthew W Hoffman, Sergio Gomez Colmenarejo, Misha Denil, Nando de Freitas, and Jascha Sohl-Dickstein. Learned optimizers that scale and generalize. In *Proceedings of the 34th International Conference on Machine Learning-Volume 70*, pages 3751–3760. JMLR. org, 2017.
- [13] Kaifeng Lv, Shunhua Jiang, and Jian Li. Learning gradient descent: Better generalization and longer horizons. In *Proceedings of the 34th International Conference on Machine Learning-Volume 70*, pages 2247–2255. JMLR. org, 2017.
- [14] Tijmen Tieleman and Geoffrey Hinton. Lecture 6.5-rmsprop: Divide the gradient by a running average of its recent magnitude. *COURSERA: Neural networks for machine learning*, 4(2): 26–31, 2012.
- [15] Diederik P. Kingma and Jimmy Ba. Adam: A method for stochastic optimization. *2015 ICLR*, arXiv preprint arXiv:1412.6980, 2015. URL <http://arxiv.org/abs/1412.6980>.
- [16] Yutian Chen, Matthew W Hoffman, Sergio Gómez Colmenarejo, Misha Denil, Timothy P Lillicrap, Matt Botvinick, and Nando de Freitas. Learning to learn without gradient descent by gradient descent. In *Proceedings of the 34th International Conference on Machine Learning-Volume 70*, pages 748–756. JMLR. org, 2017.

- [17] Yangjun Ruan, Yuanhao Xiong, Sashank Reddi, Sanjiv Kumar, and Cho-Jui Hsieh. Learning to learn by zeroth-order oracle. *ICLR*, 2020.
- [18] Yue Cao, Tianlong Chen, Zhangyang Wang, and Yang Shen. Learning to optimize in swarms. In *Advances in Neural Information Processing Systems*, pages 15018–15028, 2019.
- [19] Sijia Liu, Pin-Yu Chen, Bhavya Kailkhura, Gaoyuan Zhang, Alfred Hero, and Pramod K Varshney. A primer on zeroth-order optimization in signal processing and machine learning. *IEEE Signal Processing Magazine*, 2020.
- [20] Sachin Ravi and Hugo Larochelle. Optimization as a model for few-shot learning. 2016.
- [21] Chelsea Finn, Aravind Rajeswaran, Sham Kakade, and Sergey Levine. Online meta-learning. *arXiv preprint arXiv:1902.08438*, 2019.
- [22] Mingzhang Yin, George Tucker, Mingyuan Zhou, Sergey Levine, and Chelsea Finn. Meta-learning without memorization. In *International Conference on Learning Representations*, 2020. URL <https://openreview.net/forum?id=BklEFpEYwS>.
- [23] S. Liu, J. Chen, P.-Y. Chen, and A. O. Hero. Zeroth-order online admm: Convergence analysis and applications. In *Proceedings of the Twenty-First International Conference on Artificial Intelligence and Statistics*, volume 84, pages 288–297, April 2018.
- [24] KB Petersen, MS Pedersen, et al. The matrix cookbook, vol. 7. *Technical University of Denmark*, 15, 2008.
- [25] Ian Goodfellow, Jonathon Shlens, and Christian Szegedy. Explaining and harnessing adversarial examples. *2015 ICLR*, arXiv preprint arXiv:1412.6572, 2015.
- [26] Christian Szegedy, Wojciech Zaremba, Ilya Sutskever, Joan Bruna, Dumitru Erhan, Ian Goodfellow, and Rob Fergus. Intriguing properties of neural networks. *arXiv preprint arXiv:1312.6199*, 2013.
- [27] Nicholas Carlini and David Wagner. Towards evaluating the robustness of neural networks. In *Security and Privacy (SP), 2017 IEEE Symposium on*, pages 39–57. IEEE, 2017.
- [28] Nicolas Papernot, Ian Goodfellow, Ryan Sheatsley, Reuben Feinman, and Patrick McDaniel. cleverhans v1.0.0: an adversarial machine learning library. *arXiv preprint arXiv:1610.00768*, 2016.
- [29] Seyed-Mohsen Moosavi-Dezfooli, Alhussein Fawzi, Omar Fawzi, and Pascal Frossard. Universal adversarial perturbations. In *Proceedings of the IEEE conference on computer vision and pattern recognition*, pages 1765–1773, 2017.
- [30] Y. Lecun, L. Bottou, Y. Bengio, and P. Haffner. Gradient-based learning applied to document recognition. *Proceedings of the IEEE*, 86(11):2278–2324, Nov 1998. ISSN 0018-9219. doi: 10.1109/5.726791.
- [31] Chelsea Finn, Kelvin Xu, and Sergey Levine. Probabilistic model-agnostic meta-learning. In *Advances in Neural Information Processing Systems*, pages 9516–9527, 2018.
- [32] Erin Grant, Chelsea Finn, Sergey Levine, Trevor Darrell, and Thomas Griffiths. Recasting gradient-based meta-learning as hierarchical bayes. *ICLR*, 2018.
- [33] Aravind Rajeswaran, Chelsea Finn, Sham M Kakade, and Sergey Levine. Meta-learning with implicit gradients. In *Advances in Neural Information Processing Systems*, pages 113–124, 2019.

- [34] Hao Liu, Richard Socher, and Caiming Xiong. Taming maml: Efficient unbiased meta-reinforcement learning. In *International Conference on Machine Learning*, pages 4061–4071, 2019.
- [35] Xingyou Song, Wenbo Gao, Yuxiang Yang, Krzysztof Choromanski, Aldo Pacchiano, and Yunhao Tang. Es-maml: Simple hessian-free meta learning. *ICLR*, 2020.
- [36] Alireza Fallah, Aryan Mokhtari, and Asuman Ozdaglar. On the convergence theory of gradient-based model-agnostic meta-learning algorithms. *arXiv preprint arXiv:1908.10400*, 2019.
- [37] Kaiyi Ji, Junjie Yang, and Yingbin Liang. Multi-step model-agnostic meta-learning: Convergence and improved algorithms. *arXiv preprint arXiv:2002.07836*, 2020.
- [38] Jürgen Schmidhuber. *Evolutionary principles in self-referential learning, or on learning how to learn: the meta-meta-... hook*. PhD thesis, Technische Universität München, 1987.
- [39] Yoshua Bengio, Samy Bengio, and Jocelyn Cloutier. *Learning a synaptic learning rule*. Citeseer, 1990.
- [40] Sebastian Thrun and Lorien Pratt. *Learning to learn*. Springer Science & Business Media, 2012.
- [41] Yann LeCun et al. Lenet-5, convolutional neural networks. *URL: <http://yann.lecun.com/exdb/lenet>*, 20(5):14, 2015.
- [42] Gao Huang, Zhuang Liu, Laurens Van Der Maaten, and Kilian Q Weinberger. Densely connected convolutional networks. In *Proceedings of the IEEE conference on computer vision and pattern recognition*, pages 4700–4708, 2017.

Supplementary Material

A Gradients of MAML loss with respect to RNN parameters

Based on $G^{(k)} = \frac{\partial \theta^{(k)}}{\partial \Phi} \in \mathbb{R}^{d \times |\Phi|}$ and (3), we obtain

$$G^{(k)} = G^{(k-1)} - \frac{\partial \Delta \theta^{(k)}}{\partial \Phi}. \quad (S1)$$

For ease of presentation, we use $\text{RNN}_{\Phi}(g(\theta^{(k-1)}), \mathbf{h}_{k-1})$ to represent $\Delta \theta^{(k)} \in \mathbb{R}^d$, and the RNN output $\mathbf{h}^{(k)}$ of RNN_{Φ} is omitted when its meaning can clearly be inferred from the context. We then have

$$\frac{\partial \Delta \theta^{(k)}}{\partial \Phi} = \frac{\partial \text{RNN}_{\Phi}(g(\theta^{(k-1)}), \mathbf{h}_{k-1})}{\partial \Phi} \quad (S2)$$

$$= \frac{\partial \text{RNN}_{\Phi}(g(\theta^{(k-1)}), \mathbf{h}_{k-1})}{\partial g} \cdot \frac{\partial g(\theta^{(k-1)})}{\partial \Phi} \quad (S3)$$

$$+ \frac{\partial \text{RNN}_{\Phi}(g(\theta^{(k-1)}), \mathbf{h}_{k-1})}{\partial \mathbf{h}} \cdot \frac{\partial \mathbf{h}_{k-1}}{\partial \Phi} \quad (S4)$$

$$+ \left. \frac{\partial \text{RNN}_{\Phi}(g, \mathbf{h})}{\partial \Phi} \right|_{g=g(\theta^{(k-1)}), \mathbf{h}=\mathbf{h}_{k-1}}, \quad (S5)$$

where the equality holds by chain rule [24], \cdot denotes a matrix product that the chain rule obeys, and the term (S5) denotes the derivative w.r.t. Φ by fixing $g(\theta^{(k-1)})$ and \mathbf{h}_{k-1} as constants.

$$\frac{\partial g(\theta^{(k-1)})}{\partial \Phi} = \frac{\partial g(\theta^{(k-1)})}{\partial \theta} \cdot \frac{\partial \theta^{(k-1)}}{\partial \Phi} = \frac{\partial g(\theta^{(k-1)})}{\partial \theta} \cdot G^{(k-1)}. \quad (S6)$$

Next, we simplify the term (S4). Let $H^{(k)} = \frac{\partial \mathbf{h}_k}{\partial \Phi} \in \mathbb{R}^{|\mathbf{h}_k| \times |\Phi|}$. Note that \mathbf{h}_k depends on $\Phi, g(\theta^{(k-1)}), \mathbf{h}_{k-1}$. So we write $\mathbf{h}_k = \Pi(\Phi, g(\theta^{(k-1)}), \mathbf{h}_{k-1})$

$$\begin{aligned} H^{(k)} &= \frac{\partial \mathbf{h}_k}{\partial \Phi} = \frac{\partial}{\partial \Phi} \Pi(\Phi, g(\theta^{(k-1)}), \mathbf{h}_{k-1}) \\ &= \left. \frac{\partial \Pi(\Phi, g, \mathbf{h})}{\partial \Phi} \right|_{g=g(\theta^{(k-1)}), \mathbf{h}=\mathbf{h}_{k-1}} \\ &\quad + \frac{\partial \Pi(\Phi, g(\theta^{(k-1)}), \mathbf{h}_{k-1})}{\partial g} \cdot \frac{\partial g(\theta^{(k-1)})}{\partial \Phi} \\ &\quad + \frac{\partial \Pi(\Phi, g(\theta^{(k-1)}), \mathbf{h}_{k-1})}{\partial \mathbf{h}} \cdot \frac{\partial \mathbf{h}_{k-1}}{\partial \Phi} \\ &\stackrel{(S6)}{=} \left. \frac{\partial \Pi(\Phi, g, \mathbf{h})}{\partial \Phi} \right|_{g=g(\theta^{(k-1)}), \mathbf{h}=\mathbf{h}_{k-1}} \\ &\quad + \frac{\partial \Pi(\Phi, g(\theta^{(k-1)}), \mathbf{h}_{k-1})}{\partial g} \cdot \frac{\partial g(\theta^{(k-1)})}{\partial \theta} G^{(k-1)} \\ &\quad + \frac{\partial \Pi(\Phi, g(\theta^{(k-1)}), \mathbf{h}_{k-1})}{\partial \mathbf{h}} \cdot H^{(k-1)}. \end{aligned} \quad (S7)$$

Substituting (S6) and (S7) into (S2), we can then express (S1) as:

$$\begin{aligned} G^{(k)} &= G^{(k-1)} - \frac{\partial \text{RNN}_{\Phi}(g(\theta^{(k-1)}), \mathbf{h}_{k-1})}{\partial g} \cdot \frac{\partial g(\theta^{(k-1)})}{\partial \theta} \cdot G^{(k-1)} \\ &\quad - \frac{\partial \text{RNN}_{\Phi}(g(\theta^{(k-1)}), \mathbf{h}_{k-1})}{\partial \mathbf{h}} \cdot H^{(k-1)} \\ &\quad - \left. \frac{\partial \text{RNN}_{\Phi}(g, \mathbf{h})}{\partial \Phi} \right|_{g=g(\theta^{(k-1)}), \mathbf{h}=\mathbf{h}_{k-1}}, \end{aligned} \quad (S8)$$

where $H^{(k-1)}$ is determined by the recursion (S7).

It is clear from (S7) and (S8) that the second order derivative would at most be involved due to the presence of $\frac{\partial g(\boldsymbol{\theta}^{(k-1)})}{\partial \boldsymbol{\theta}}$ if $g(\boldsymbol{\theta}^{(k-1)})$ is specified by the first-order derivative w.r.t. $\boldsymbol{\theta}$. By contrast, if it is specified by the ZO gradient estimate, then there will only be first-order derivatives involved in (S7) and (S8). Lastly, we remark that the recursive forms of (S7) and (S8) facilitate our computation, and $G^{(0)} = 0$ and $H^{(0)} = 0$.

B Proof of Theorem 1

Before showing the theoretical results, we first give the following a blanket of assumptions.

B.1 Assumptions

In practice, the size of data and variables are limited and the function is also bounded. To proceed, we have the following standard assumptions for quantifying the gradient difference between L2O and LFT.

A1. We assume that gradient estimate is unbiased, i.e.,

$$\left[\frac{1}{N} \sum_{i=1}^N \mathbb{E}_{\mathcal{D}_i} \nabla_{\boldsymbol{\theta}_i} f_i(\boldsymbol{\theta}_i^{(k)}; \mathcal{D}_i) \right] = \frac{1}{N} \sum_{i=1}^N \nabla_{\boldsymbol{\theta}_i} f_i(\boldsymbol{\theta}_i^{(k)}) := \nabla_{\boldsymbol{\theta}} f(\boldsymbol{\theta}_1^{(k)}, \dots, \boldsymbol{\theta}_N^{(k)}), \forall k, \quad (\text{S9})$$

where \mathcal{D}_i denotes the training/validation data sample of the i th task, and $\boldsymbol{\theta}$ stands for $\boldsymbol{\theta}_1, \dots, \boldsymbol{\theta}_N$.

A2. We assume that the gradient estimate has bounded variance for both $\mathcal{D}_i^{\text{tr}}, \mathcal{D}_i^{\text{val}}, \forall i, k$, i.e.,

$$\mathbb{E}_{\mathcal{D}_i^{(\cdot)}} \left[\left\| \nabla_{\boldsymbol{\theta}_i} f_i(\boldsymbol{\theta}_i^{(k)}; \mathcal{D}_i) - \nabla_{\boldsymbol{\theta}} f(\boldsymbol{\theta}_1^{(k)}, \dots, \boldsymbol{\theta}_N^{(k)}) \right\|^2 \right] \leq \sigma^2, \forall i, k. \quad (\text{S10})$$

The same assumption is also applied for $\partial \boldsymbol{\theta}_i^{(k)} / \partial \boldsymbol{\Phi}$:

$$\mathbb{E} \left[\frac{1}{N} \sum_{i=1}^N \frac{\partial(\boldsymbol{\theta}_i^{(k)}; \mathcal{D}_i)}{\partial \boldsymbol{\Phi}} \right] = \frac{1}{N} \sum_{i=1}^N \frac{\partial \boldsymbol{\theta}_i^{(k)}}{\partial \boldsymbol{\Phi}} := \frac{\partial f(\boldsymbol{\theta}_1^{(k)}, \dots, \boldsymbol{\theta}_N^{(k)})}{\partial \boldsymbol{\Phi}}, \forall i, k, \quad (\text{S11})$$

$$\mathbb{E} \left[\left\| \frac{\partial(\boldsymbol{\theta}_i^{(k)}; \mathcal{D}_i)}{\partial \boldsymbol{\Phi}} - \frac{\partial f(\boldsymbol{\theta}_1^{(k)}, \dots, \boldsymbol{\theta}_N^{(k)})}{\partial \boldsymbol{\Phi}} \right\|^2 \right] \leq \sigma^2, \forall i, k. \quad (\text{S12})$$

A3. We assume that the size of gradient is uniformly upper bounded, i.e., $\mathbb{E} \|\nabla f_i(\boldsymbol{\theta}_i^{(k)}, \mathcal{D}_i^{(\cdot)})\| \leq G$, $\mathbb{E} \left\| \frac{\partial(\boldsymbol{\theta}_i^{(k)}, \mathcal{D}_i^{(\cdot)})}{\partial \boldsymbol{\Phi}} \right\| \leq G, \forall i, k$.

Proof. Assume that A1–A3 hold. Let $w_k = \frac{1}{K}$. From the definitions of $F(\boldsymbol{\Phi})$ and $\widehat{F}(\boldsymbol{\Phi})$, we have

$$\begin{aligned} & \|\nabla_{\boldsymbol{\Phi}} \widehat{F}(\boldsymbol{\Phi}) - \nabla_{\boldsymbol{\Phi}} F(\boldsymbol{\Phi})\|^2 \\ &= \left\| \frac{1}{N} \sum_{i=1}^N \frac{1}{K} \sum_{k=1}^K \mathbb{E}_{\mathcal{D}_i^{\text{tr}} \mathcal{D}_i^{\text{val}}} \nabla_{\boldsymbol{\Phi}} f(\boldsymbol{\theta}_i^{(k)}; \mathcal{D}_i^{\text{val}}) - \nabla_{\boldsymbol{\Phi}} f(\boldsymbol{\theta}_1^{(k)}, \dots, \boldsymbol{\theta}_N^{(k)}) \right\|^2 \end{aligned} \quad (\text{S13})$$

$$\stackrel{\text{(a)}}{\leq} \frac{1}{K} \sum_{k=1}^K \left\| \mathbb{E}_{\mathcal{D}_i^{\text{tr}} \mathcal{D}_i^{\text{val}}} \frac{1}{N} \sum_{i=1}^N \nabla_{\boldsymbol{\Phi}} f(\boldsymbol{\theta}_i^{(k)}; \mathcal{D}_i^{\text{val}}) - \nabla_{\boldsymbol{\Phi}} f(\boldsymbol{\theta}_1^{(k)}, \dots, \boldsymbol{\theta}_N^{(k)}) \right\|^2 \quad (\text{S14})$$

$$\stackrel{\text{(b)}}{\leq} \frac{1}{K} \sum_{k=1}^K \left\| \frac{1}{N} \sum_{i=1}^N \mathbb{E}_{\mathcal{D}_i^{\text{tr}} \mathcal{D}_i^{\text{val}}} \nabla_{\boldsymbol{\Phi}} f(\boldsymbol{\theta}_i^{(k)}; \mathcal{D}_i^{\text{val}}) - \nabla_{\boldsymbol{\Phi}} f(\boldsymbol{\theta}_1^{(k)}, \dots, \boldsymbol{\theta}_N^{(k)}) \right\|^2 \quad (\text{S15})$$

$$\stackrel{\text{(c)}}{\leq} \frac{1}{K} \sum_{k=1}^K \left\| \frac{1}{N} \sum_{i=1}^N \mathbb{E}_{\mathcal{D}_i^{\text{tr}} \mathcal{D}_i^{\text{val}}} \frac{\partial f(\boldsymbol{\theta}_i^{(k)}; \mathcal{D}_i^{\text{val}})}{\partial \boldsymbol{\theta}_i^{(k)}} \frac{\partial(\boldsymbol{\theta}_i^{(k)}; \mathcal{D}_i^{\text{tr}})}{\partial \boldsymbol{\Phi}} - \nabla_{\boldsymbol{\Phi}} f(\boldsymbol{\theta}_1^{(k)}, \dots, \boldsymbol{\theta}_N^{(k)}) \right\|^2 \quad (\text{S16})$$

$$\begin{aligned} & \leq \frac{1}{K} \sum_{k=1}^K \frac{1}{N} \sum_{i=1}^N \left\| \mathbb{E}_{\mathcal{D}_i^{\text{tr}} \mathcal{D}_i^{\text{val}}} \frac{\partial f(\boldsymbol{\theta}_i^{(k)}; \mathcal{D}_i^{\text{val}})}{\partial \boldsymbol{\theta}_i^{(k)}} \frac{\partial(\boldsymbol{\theta}_i^{(k)}; \mathcal{D}_i^{\text{tr}})}{\partial \boldsymbol{\Phi}} - \frac{\partial f(\boldsymbol{\theta}_1^{(k)}, \dots, \boldsymbol{\theta}_N^{(k)})}{\partial \boldsymbol{\theta}_i^{(k)}} \frac{\partial(\boldsymbol{\theta}_i^{(k)}; \mathcal{D}_i^{\text{tr}})}{\partial \boldsymbol{\Phi}} \right. \\ & \quad \left. + \frac{\partial f(\boldsymbol{\theta}_1^{(k)}, \dots, \boldsymbol{\theta}_N^{(k)})}{\partial \boldsymbol{\theta}_i^{(k)}} \frac{\partial(\boldsymbol{\theta}_i^{(k)}; \mathcal{D}_i^{\text{tr}})}{\partial \boldsymbol{\Phi}} - \nabla_{\boldsymbol{\Phi}} f(\boldsymbol{\theta}_1^{(k)}, \dots, \boldsymbol{\theta}_N^{(k)}) \right\|^2 \end{aligned} \quad (\text{S17})$$

$$\stackrel{\text{(d)}}{\leq} \frac{2G^2}{K} \sum_{k=1}^K \left(\frac{\sigma^2}{D_{\text{val}}} + \frac{\sigma^2}{D_{\text{tr}}} \right) \quad (\text{S18})$$

$$\leq 2G^2 \sigma^2 \left(\frac{1}{D_{\text{val}}} + \frac{1}{D_{\text{tr}}} \right) \quad (\text{S19})$$

where in (a) we use Jensen's inequality, in (b) we apply the triangle inequality, in (c) we use the chain rule, (d) is true because

$$\begin{aligned} & \left\| \mathbb{E}_{\mathcal{D}_i^{\text{tr}} \mathcal{D}_i^{\text{val}}} \frac{\partial f(\boldsymbol{\theta}_i^{(k)}; \mathcal{D}_i^{\text{val}})}{\partial \boldsymbol{\theta}_i^{(k)}} \frac{\partial(\boldsymbol{\theta}_i^{(k)}; \mathcal{D}_i^{\text{tr}})}{\partial \boldsymbol{\Phi}} - \frac{\partial f(\boldsymbol{\theta}_1^{(k)}, \dots, \boldsymbol{\theta}_N^{(k)})}{\partial \boldsymbol{\theta}_i^{(k)}} \frac{\partial(\boldsymbol{\theta}_i^{(k)}; \mathcal{D}_i^{\text{tr}})}{\partial \boldsymbol{\Phi}} \right\|^2 \\ & \stackrel{\text{(i)}}{\leq} \left\| \mathbb{E}_{\mathcal{D}_i^{\text{val}}} \mathbb{E}_{\mathcal{D}_i^{\text{tr}} | \mathcal{D}_i^{\text{val}}} \frac{\partial(\boldsymbol{\theta}_i^{(k)}; \mathcal{D}_i^{\text{tr}})}{\partial \boldsymbol{\Phi}} \right\|^2 \left\| \mathbb{E}_{\mathcal{D}_i^{\text{tr}}} \mathbb{E}_{\mathcal{D}_i^{\text{val}} | \mathcal{D}_i^{\text{tr}}} \frac{\partial f(\boldsymbol{\theta}_i^{(k)}; \mathcal{D}_i^{\text{val}})}{\partial \boldsymbol{\theta}_i^{(k)}} - \frac{\partial f(\boldsymbol{\theta}_1^{(k)}, \dots, \boldsymbol{\theta}_N^{(k)})}{\partial \boldsymbol{\theta}_i^{(k)}} \right\|^2 \end{aligned} \quad (\text{S20})$$

$$\stackrel{\text{(ii)}}{\leq} G^2 \mathbb{E}_{\mathcal{D}_i^{\text{tr}}} \mathbb{E}_{\mathcal{D}_i^{\text{val}} | \mathcal{D}_i^{\text{tr}}} \left\| \frac{\partial f(\boldsymbol{\theta}_i^{(k)}; \mathcal{D}_i^{\text{val}})}{\partial \boldsymbol{\theta}_i^{(k)}} - \frac{\partial f(\boldsymbol{\theta}_1^{(k)}, \dots, \boldsymbol{\theta}_N^{(k)})}{\partial \boldsymbol{\theta}_i^{(k)}} \right\|^2 \quad (\text{S21})$$

$$\leq \frac{G^2 \sigma^2}{D_{\text{val}}} \quad (\text{S22})$$

where in (i) we use Cauchy-Schwarz inequality, in (ii) we use Jensen's inequality; and similarly we

have

$$\begin{aligned} & \left\| \mathbb{E}_{\mathcal{D}_i^{\text{tr}} \mathcal{D}_i^{\text{val}}} \frac{\partial f(\boldsymbol{\theta}_1^{(k)}, \dots, \boldsymbol{\theta}_N^{(k)})}{\partial \boldsymbol{\theta}_i^{(k)}} \frac{\partial(\boldsymbol{\theta}_i^{(k)}, \mathcal{D}_i^{\text{tr}})}{\partial \boldsymbol{\Phi}} - \nabla_{\boldsymbol{\Phi}} f(\boldsymbol{\theta}_1^{(k)}, \dots, \boldsymbol{\theta}_N^{(k)}) \right\|^2 \\ & \leq \left\| \mathbb{E}_{\mathcal{D}_i^{\text{tr}}} \frac{\partial f(\boldsymbol{\theta}_1^{(k)}, \dots, \boldsymbol{\theta}_N^{(k)})}{\partial \boldsymbol{\theta}_i^{(k)}} \left(\frac{\partial(\boldsymbol{\theta}_i^{(k)}, \mathcal{D}_i^{\text{tr}})}{\partial \boldsymbol{\Phi}} - \frac{\partial f(\boldsymbol{\theta}_1^{(k)}, \dots, \boldsymbol{\theta}_N^{(k)})}{\partial \boldsymbol{\Phi}} \right) \right\|^2 \end{aligned} \quad (\text{S23})$$

$$\leq \left\| \frac{\partial f(\boldsymbol{\theta}_1^{(k)}, \dots, \boldsymbol{\theta}_N^{(k)})}{\partial \boldsymbol{\theta}_i^{(k)}} \right\|^2 \left\| \mathbb{E}_{\mathcal{D}_i^{\text{tr}}} \frac{\partial(\boldsymbol{\theta}_i^{(k)}, \mathcal{D}_i^{\text{tr}})}{\partial \boldsymbol{\Phi}} - \frac{\partial f(\boldsymbol{\theta}_1^{(k)}, \dots, \boldsymbol{\theta}_N^{(k)})}{\partial \boldsymbol{\Phi}} \right\|^2 \quad (\text{S24})$$

$$\leq G^2 \mathbb{E}_{\mathcal{D}_i^{\text{tr}}} \left\| \frac{\partial(\boldsymbol{\theta}_i^{(k)}, \mathcal{D}_i^{\text{tr}})}{\partial \boldsymbol{\Phi}} - \frac{\partial f(\boldsymbol{\theta}_1^{(k)}, \dots, \boldsymbol{\theta}_N^{(k)})}{\partial \boldsymbol{\Phi}} \right\|^2 \quad (\text{S25})$$

$$\leq \frac{G^2 \sigma^2}{D_{\text{tr}}}. \quad (\text{S26})$$

Then, we can have

$$\|\nabla_{\boldsymbol{\Phi}} F(\boldsymbol{\Phi}) - \nabla_{\boldsymbol{\Phi}} \widehat{F}(\boldsymbol{\Phi})\| \leq \sqrt{2} G \sigma \sqrt{\frac{1}{D_{\text{tr}}} + \frac{1}{D_{\text{val}}}} \sim \mathcal{O} \left(\underbrace{\sqrt{\frac{1}{D_{\text{tr}}} + \frac{1}{D_{\text{val}}}}}_{\epsilon(D_{\text{tr}}, D_{\text{val}})} \right). \quad (\text{S27})$$

Therefore, it is shown that when D_{tr} and D_{val} are both large, then the difference between $\nabla_{\boldsymbol{\Phi}} F(\boldsymbol{\Phi})$ and $\nabla_{\boldsymbol{\Phi}} \widehat{F}(\boldsymbol{\Phi})$ are quite small. If we assume that L2O converges to the stationary points in the sense the L2O algorithm is able to find a good solution for equation (9) in the main paper by optimizing $\boldsymbol{\Phi}$, then it is implied that our approach will also converge to the stationary point up some error, i.e., $\epsilon(D_{\text{tr}}, D_{\text{val}})$ which is small. \blacksquare

C Experiment Setup for UAP

L2O is trained with 1000 few-shot classification tasks. During training, we set $\mathcal{D}_i^{\text{val}} = \mathcal{D}_i^{\text{tr}}$ as L2O does not have a separate meta-validation set as in LFT and MAML. The L2O has the same RNN architecture as the LFT. MAML is also trained with 1000 tasks but aims to acquire a good initialization $\boldsymbol{\theta}$ so that it can quickly adapt to new tasks.

RNN Architecture A one-layer LSTM RNN model with 10 hidden units is utilized in our experiments. Besides, we use one additional linear layer to project the RNN hidden state to the output. ADAM is applied with an initial learning rate of 0.001 to train the proposed methods with the truncated backpropagation through time (BPTT). We unroll the RNN for 20 steps and run the optimization for 200 steps during training.

D ℓ_1 norm of UAP learnt by LFT, L2O and MAML

Figure A1 shows ℓ_1 norm of UAP learnt by LFT, L2O and MAML in various training and evaluation scenarios. In general, the ℓ_1 norm of the UAP learnt by LFT is smaller than that of using L2O, except the case (MNIST, MNIST+CIFAR10). However, we recall from Figure 1 that the ASR obtained by L2O is much poorer than LFT in the case (MNIST, MNIST+CIFAR10).

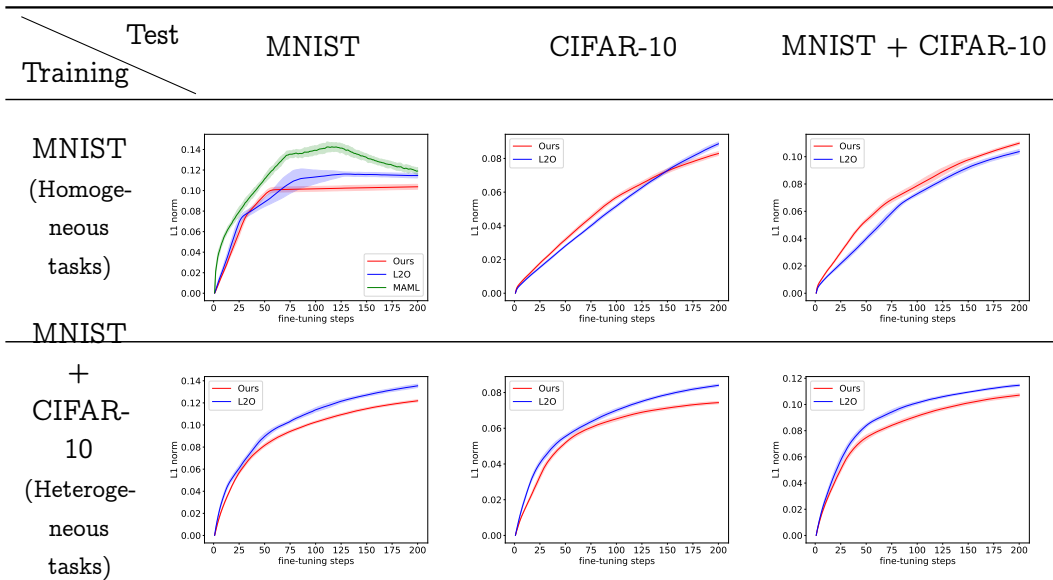


Figure A1: Perturbation strength of UAP (ℓ_1 norm) learnt by LFT (ours), MAML, L2O in various training and evaluation scenarios. The settings are consistent with Figure 1.

E Additional Experiments on UAP

Figure A2 presents the fine-tuning loss of the UAP learnt by LFT, L2O and MAML in various training and evaluation scenarios. As expected, LFT yields a fast adaptation of UAP to attack unseen test images, corresponding to the lowest fine-tuning loss.

In Figure A3, we compare the ASR and ℓ_1 perturbation strength of UAP generated by LFT with those of projected gradient descent (PGD) universal attacks. The LFT model is trained on MNIST and tested on CIFAR-10. And PGD is applied to generating UAP on \mathcal{D}^{tr} (CIFAR-10), and we then test the obtained UAP on \mathcal{D}^{val} (CIFAR-10). As we can see, UAP generated by PGD has much worse attack transferability than LFT. Surprisingly, although LFT is trained over MNIST, it yields an UAP generator with great transferability to a different dataset CIFAR-10.

In Figure A4, we visualize the patterns of UAP generated by LFT, L2O, MAML and PGD under MNIST.

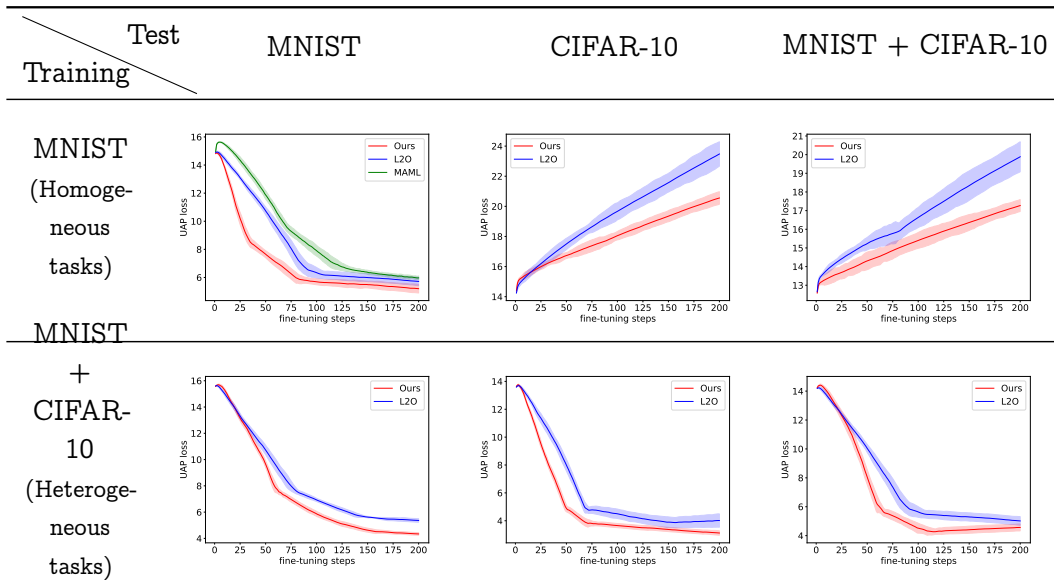


Figure A2: Fine-tuning loss of UAP learnt by LFT, MAML, L2O in various training and evaluation scenarios. The settings are consistent with Figure 1.

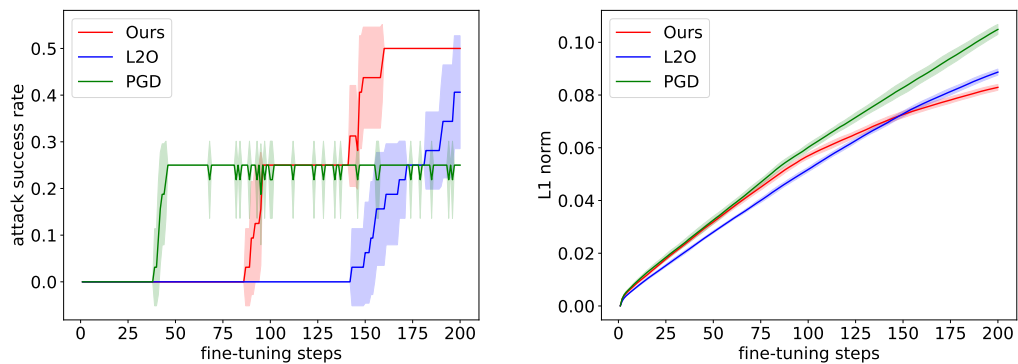


Figure A3: Comparison between UAP learnt by LFT and that learnt by PGD. (Left) Attack success rate (ASR) versus fine-tuning steps. (Right) ℓ_1 perturbation strength.

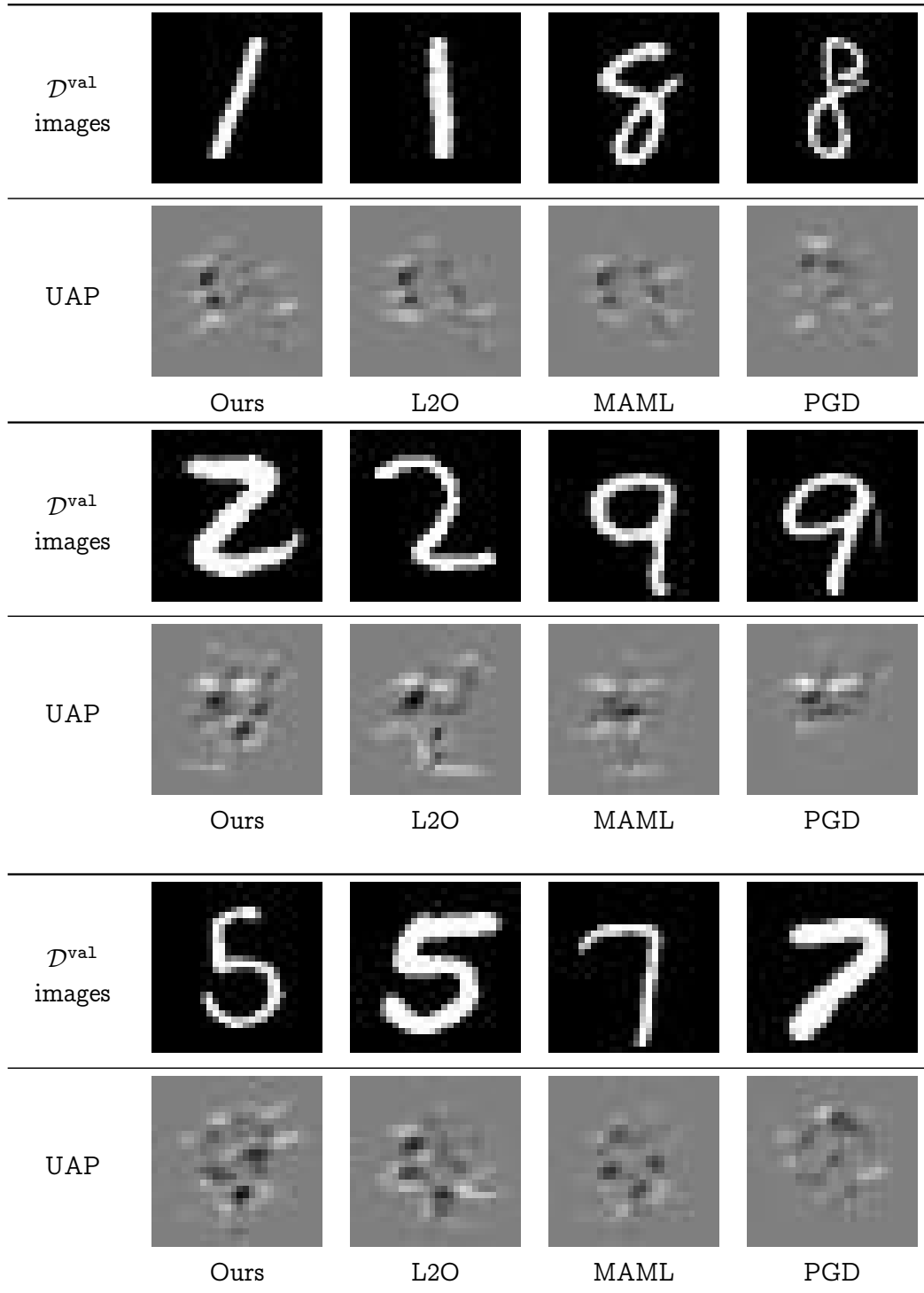


Figure A4: Visualization of UAP patterns generated by LFT (ours), MAML, L2O and PGD under MNIST. The row ' \mathcal{D}^{val} images' denotes the multiple images used as a validation set at testing. The row 'UAP' denotes the universal perturbation patterns generated by different optimizers.

F Additional Experiments in Few-Shot Classification

In Table A1, we show the accuracy of LFT at various few-shot configurations, namely, k-shot 2-way under CIFAR-10 for $k \in \{1, 3, 5, 10\}$. We observe that as the number of samples increases, the gain of testing accuracy increases. Surprisingly, even in the 1-shot case, LFT still achieves 45% accuracy, demonstrating its power in the few-shot learning. Moreover, we observe that the improvement of LFT over L2O advances as the number of learning samples decreases. This observation is consistent with our theoretical results in Theorem 1, showing that the size of the meta-training dataset would be a key factor to measure the difference of the gradients of the objective functions between L2O and LFT. And accordingly, it yields different meta model solutions in the few-shot learning regime.

Table A1: Accuracy of LFT for various few-shot configurations on CIFAR-10.

	1 shot	3 shot	5 shot	10 shot
L2O 2-way	27%	49%	63%	69%
LFT 2-way	45%	57%	66%	71%

Furthermore, in Table A2, we compare LFT with L2O and MAML for tackling 5-way 5-shot congruous/incongruous tasks defined over Omniglot and MiniImagenet. We assign two CNN models to Omniglot- and MiniImagenet-related tasks: CNN with 2 CONV layers for Omniglot tasks, and CNN with 4 CONV layers for MiniImagenet tasks. See Appendix H for detailed distinction between meta-learning for congruous tasks and meta-learning for incongruous task. As we can see, LFT outperforms L2O and MAML in the congruous setting (Omniglot, Omniglot) as well as the other incongruous task settings. It is worth mentioning that the accuracy of MAML (93%) is lower than that of the accuracy (98%) reported in [2] since a different CNN architecture is considered in our experiments.

Table A2: Averaged test accuracy \pm standard deviation for different classifiers acquired from different meta-learners, MAML, L2O, and our proposed LFT, in each paired meta-training and testing configuration. Here the merged ‘Training’ columns show training data sources (implying different model architectures – CNN with 2 CONV layers for Omniglot tasks & CNN with 4 CONV layers for MiniImagenet tasks) and meta-learning methods. Similarly, the merged ‘Testing’ rows show data sources of test tasks as well as the associated model architectures. Note that MAML is *not applicable* (N/A) to incongruous tasks across multiple architectures and datasets.

		Testing		
		Omniglot	MiniImagenet	Omniglot + MiniImagenet
Omniglot	MAML	93% \pm 0.7%	N/A	N/A
	L2O	89% \pm 0.9%	17% \pm 1.8%	42% \pm 1.7%
	LFT	94% \pm 0.8%	19% \pm 2.1%	46% \pm 1.4%
Omniglot + MiniImagenet	MAML	N/A	N/A	N/A
	L2O	85% \pm 1.3%	41% \pm 1.8%	57% \pm 1.5%
	LFT	89% \pm 1.0%	45% \pm 1.9%	62% \pm 1.4%

G Experiment Setup for Regression

We first introduce multiple tasks, each of which involves regressing from the input to the output of a sine wave, where the amplitude A and the phase of the sinusoid ξ are varied between tasks, as shown

below,

$$z_j^{(i)} = A^{(i)} \sin(r_j^{(i)} + \xi^{(i)}), j \in [K] \quad (\text{S28})$$

where K is the number of observations at the i -th task, $r_j^{(i)}$ is randomly drawn from $[-5, 5]$, $A^{(i)}$ is randomly drawn from $[0.1, 5]$, and $\xi^{(i)}$ is randomly drawn from $[0, \pi]$. For the i -th task, we generate $(\mathcal{D}_i^{\text{tr}}, \mathcal{D}_i^{\text{val}})$ where $\mathcal{D}_i^{\text{tr}} = \{r_j^{(i)}, z_j^{(i)}\}$, and $\mathcal{D}_i^{\text{val}} = \{r_{j'}^{(i)}, z_{j'}^{(i)}\}$ drawn from the same task function. Considering a regressor $r(\theta; r_j^{(i)})$ as a neural network with 2 hidden layers with ReLU nonlinearities, the task i -specified loss is given by

$$f_i(\theta) = \sum_{j=1}^K [r(\theta; r_j^{(i)}) - z_j^{(i)}]^2, \quad (\text{S29})$$

where θ is the regression coefficient. We would like to find the best regressor to have fast adaptation to a new task.

RNN Architecture In LFT and L2O, we use a LSTM model to find the regressor coefficient θ . The LSTM RNN model has one-layer with 10 hidden units. Besides, we use one additional linear layer to project the RNN hidden state to the output. ADAM is applied with an initial learning rate of 0.001 to train the proposed methods with BPTT. We unroll the RNN for 20 steps and run the optimization for 200 steps during training.

H Visual comparison of meta-learning for congruous and incongruous tasks

This section provides visual depiction of the meta-learning problem considered in Appendix F. We wish to emphasize the difference between the meta-learning and the subsequent “meta-testing” done with MAML and our proposed meta-learning.

In MAML, for any few-shot learning task \mathcal{T}_i with data sets $\mathcal{D}_i^{\text{tr}}$ of learning task specific parameters/optimizee θ_i , the meta-learning is performed over a parameter/optimizee θ shared by all tasks that is selected as the initial value for $\theta_i \forall i$. As a specific example depicted in Figure A5, *congruous* few shot tasks would correspond to 3-way 4-shot digit classification with MNIST images and the task specific parameters/optimizee θ_i corresponds to the model parameters of the task-specific LeNet, while the meta-learned parameter/optimizee θ correspond the LeNet parameters shared by all tasks as the initial model parameters to be fine-tuned at “meta-test” time. For the meta-learning of θ , the task-specific meta-gradients $\nabla_{\theta} f_i$ from \mathcal{T}_i are used to update the meta-learned θ .

We consider meta-learning across *incongruous* few shot tasks. We are still considering few-shot learning tasks \mathcal{T}_i with data sets $\mathcal{D}_i^{\text{tr}}$ of learning task-specific parameters/optimizee θ_i but *it is not possible to meta-learn a single shared initialization θ or use a single shared parameter/optimizee initialization across different tasks at meta-test time*. Consider the incongruous few-shot digits classification tasks in Figure A6 – each task \mathcal{T}_i with data $\mathcal{D}_i^{\text{tr}}$ corresponds to learning the task-specific parameters/optimizee θ_i corresponding to different models – models with LeNet architecture for tasks generated from the MNIST images and models with DenseNet architecture for the tasks generated from SVHN images. As emphasized by the different colored outlines for the per-task models in Figure A6, we would like to note that there is no sharing of model parameters (as initialization or otherwise) between task specific optimizees θ_i – each of these task-specific model parameters/optimizees θ_i are fine-tuned by the meta-learned RNN optimizer *from a random initialization*.

The task-specific learning is done with the task-specific gradients $\nabla_{\theta_i} f_i$. In L2O (learning to optimize) and our proposed meta-learning scheme, we meta-learn the parameters ϕ of a RNN based learned-optimizer and that is the shared optimizer across all tasks during meta-learning and meta-testing. For meta-learning ϕ , the task-specific meta-gradients $\nabla_{\phi} f_i$ from \mathcal{T}_i are used. In L2O, these

meta-gradients are generated with $\mathcal{D}_i^{\text{tr}}$ while our proposed scheme utilizes $\mathcal{D}_i^{\text{val}}$ to compute these meta-gradients.

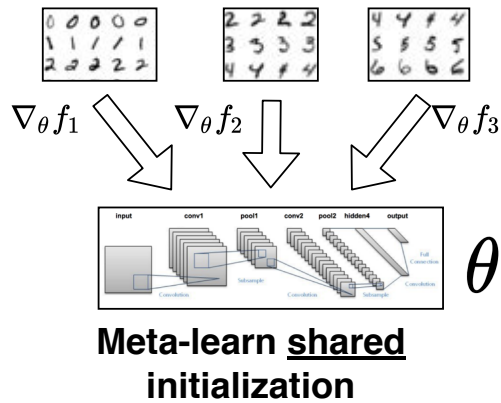


Figure A5: *Model agnostic meta-learning with congruous few-shot tasks.* The meta-learned parameters θ of the deep learning LeNet-5 [41] model is shared by all congruous few-shot MNIST digit classification tasks $\mathcal{T}_1, \mathcal{T}_2, \mathcal{T}_3$ as the initial value for the task specific LeNet-5 model parameters $\theta_1, \theta_2, \theta_3$ respectively for task-specific fine-tuning at meta-test time. The meta-learning of the shared parameter/optimizee θ uses task-specific meta-gradients $\nabla_{\theta} f_i = \partial f_i / \partial \theta$ of task-specific objectives f_i w.r.t. the meta-learned parameter θ shared across all congruous tasks.

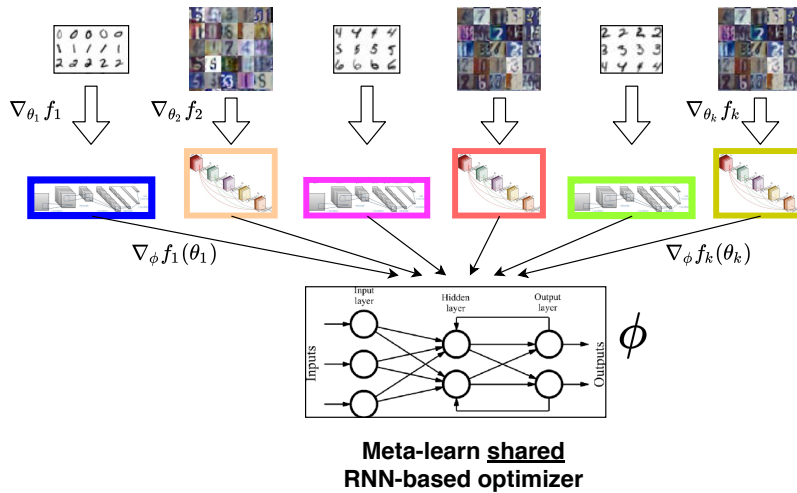


Figure A6: *Our proposed $\mathcal{L}2\mathcal{O}$ meta-learning setup with incongruous tasks.* The meta-learned RNN optimizer parameters Φ are shared by all incongruous digit classification tasks $\mathcal{T}_1, \dots, \mathcal{T}_k$ to fine-tune the task specific optimizers $\theta_1, \dots, \theta_k$ respectively with task specific gradients $\nabla_{\theta_i} f_i = \partial f_i / \partial \theta_i, i \in [k]$ at meta-learning and meta-test time. For few-shot tasks based on MNIST images, we may use the LeNet-5 [41] architecture based models; for few-shot tasks based on SVHN images, we may use the DenseNet [42] architecture based models. The different colored outlines around each of the task-specific models emphasize that there is no sharing of model parameters between these tasks – each of these task-specific model parameters/optimizers θ_i are fine-tuned by the meta-learned RNN optimizer from a random initialization. The meta-learning of the shared RNN optimizer Φ uses the task-specific meta-gradients $\nabla_{\Phi} f_i = \partial f_i / \partial \Phi = (\partial f_i / \partial \theta_i) \cdot (\partial \theta_i / \partial \Phi), i \in [k]$. Note that MAML cannot be applied in this incongruous setting to meta-learn a model parameter/optimizer initialization that can be used to initialize the optimizer for all tasks.